Acta Crystallographica Section B
Structural Science
ISSN 0108-7681

Structures of $[Pd(NH_3)_2X_2]$ and its chemical transformation in the solid state

S. D. Kirik,[a]* L. A. Solovyov,[a] A. I. Blokhin[b] and I. S. Yakimov[b]

[a]Institute of Chemistry and Chemical Technology, Academy of Sciences, 660049 Krasnoyarsk, Russia, and [b]Academy of Non-ferrous Metals and Gold, 660049 Krasnoyarsk, Russia

Correspondence e-mail: kirik@icct.krsk.infotel.ru

Received 22 September 1999
Accepted 5 January 2000

Crystal structures of $[Pd(NH_3)_2X_2]$ complexes, where X = Br or I, diamminediiodo-/-dibromopalladium(II), have been studied by X-ray powder diffraction. The series consists of five complexes: *cis*-$[Pd(NH_3)_2Br_2]$ (I) [a = 13.3202 (7), b = 12.7223 (6), c = 7.05854 (3) Å, Z = 8, space group *Pbca*], *trans*-$[Pd(NH_3)_2Br_2]$ (II) [a = 6.7854 (3), b = 7.1057 (3), c = 6.6241 (2) Å, α = 103.221 (3), β = 102.514 (2), γ = 100.386 (3)°, Z = 2, space group $P\bar{1}$], *β-trans*-$[Pd(NH_3)_2Br_2]$ (III) [a = 8.4315 (3), b = 8.4206 (3), c = 8.0916 (2) Å, Z = 4, space group *Pbca*], *cis*-$[Pd(NH_3)_2I_2]$ (IV) [a = 13.9060 (8), b = 13.5035 (8), c = 7.5050 (4) Å, Z = 8, space group *Pbca*], and *β-trans*-$[Pd(NH_3)_2I_2]$ (V) [a = 8.8347 (5), b = 8.8410 (5), c = 8.6081 (2) Å, Z = 4, space group *Pbca*]. Patterson synthesis and Rietveld refinement have been used for structural determination. Molecular structures with column- or parquet-type packing of flat complexes are characteristic of these substances. Corresponding *cis*- and *β-trans* compounds are isostructural. The thermal transformations *cis*→*trans*→*β-trans* (*cis*→*β-trans* in the case of iodine) are considered. Cl derivatives are also discussed. The transformations proceed irreversibly and are accompanied by decreasing specific volume. Owing to these features, they can be classified as chemical reactions. High-temperature X-ray powder diffraction was used to study the transformations in air. The set of data is consistent with a solid state transformation from *cis* to *trans*. According to this model, the columns of molecules remain intact during the process, and the transformation proceeds *via* the breaking of Pd···X and Pd···N intermolecular bonds. The powder diffraction data have been deposited in ICDD-JCPDS (45-0596, 46-0876, 46-0879, 47-1690, 48-1185).

1. Introduction

The compounds of $[Pd(NH_3)_2X_2]$, where X = Cl, Br, I, are known as good models for studying the electronic structure and features of chemical bonding as well as the thermodynamic properties of coordination compounds. These compounds could provide important information on the long-length scale-axial coordination affinity of metals, observed for many Pt^{II} and Pd^{II} coordination compounds and revealed in many chemical processes. Unfortunately, there is a shortage of structural information, which limits the application of theoretical approaches for predicting the chemical properties and behaviour of these compounds. Basically, this results from a lack of single crystals for the most interesting complexes. There are just two sets of structural data for related substances, namely, for *cis*- and *trans*-$[Pt(NH_3)_2Cl_2]$ (Porai-Koshits, 1954; Milburn & Truter, 1966). It should be noted that

for the *cis* configuration, the crystal structure has been determined only for the low-temperature modification (α-phase), while the commercially available β-form is still not determined. More recently, crystal structure data for $[Pd(NH_3)_2Cl_2]$ were published (Kirik *et al.*, 1996). In this paper we present the crystal structure data for the other members of the $[Pd(NH_3)_2(halide)_2]$ series as well as data on the structural transformation of these compounds. Three phases, the *cis, trans* and β-*trans* modifications for X = Br, were prepared and investigated. For iodine we were able to obtain only two, the *cis* and β-*trans* compounds. Thermally induced phase transformations were studied by high-temperature X-ray diffraction.

2. Experimental

2.1. Material preparation

The syntheses of *cis*-$[Pd(NH_3)_2X_2]$, where X = Br or I, were carried out using the so-called mechanical–chemical approach that gave good results in the case of the Cl derivatives (Kirik *et al.*, 1996). The starting substance, $[Pd(NH_3)_2C_2O_4]$ was placed in an agate mortar, and HBr or HI was added in excess of 10–20%. The mixture was ground until the colour of the substance changed from pale yellow to bright orange. After washing and drying the solid was obtained. *trans*-$[Pd(NH_3)_2Br_2]$ was obtained by mild thermal transformation of *cis*-$[Pd(NH_3)_2Br_2]$ using water. The initial substance was placed in the water and heated at 320–330 K for 2–3 h. Owing to its low solubility, the substance remained in a slurry during this procedure. The same approach was applied to the preparation of β-*trans* isomers at 360 K.

Iodine derivatives are less stable than the bromide ones. They were prepared at temperatures close to 273 K. The *cis* isomer transforms into the *trans* one in the presence of trace amounts of moisture at room temperature. *trans*-$[Pd(NH_3)_2I_2]$ was not obtained as a pure phase but it was observed in a mixture of products. More details on the material preparation will be published later.

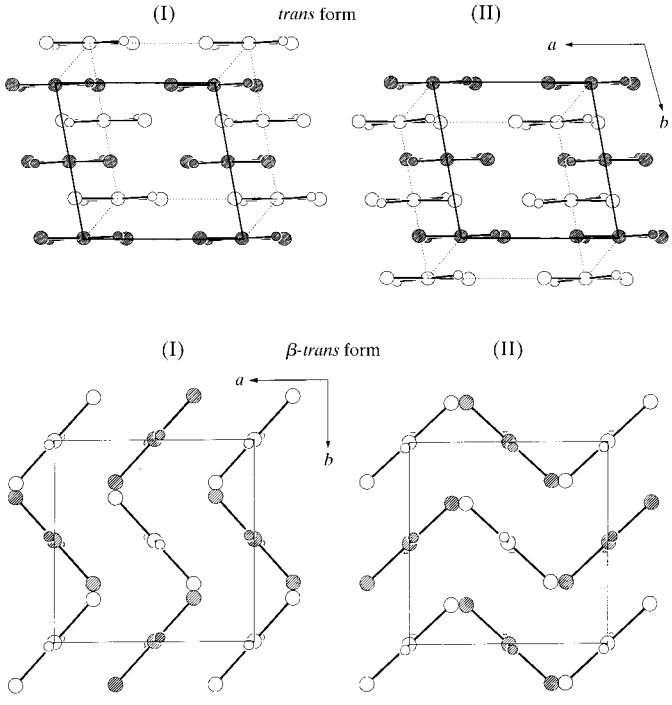

Figure 1
Two different types of stacking (I and II) of layers of complexes parallel to the (001) plane in *trans*- and β-*trans*-$[Pd(NH_3)_2(halide)_2]$. The projections of the structure on the (001) plane are shown. The complexes at different levels have different shading.

2.2. X-ray powder diffraction structural investigations

Powder diffraction data were collected using a DRON-4 diffractometer in Bragg–Brentano geometry with sample spinner, flat-graphite secondary monochromator and scintillation counter. The measurements were taken using Cu $K\alpha$ radiation at room temperature in air. Peak positions for the unit-cell determination were measured after smoothing and $K\alpha_2$ stripping. The unit-cell parameters were found and refined with the assistance of indexing programs (Visser, 1969; Kirik *et al.*, 1979). The powder diffraction data have been deposited in ICDD–JCPDS (45-0596, 46-0876, 46-0879, 47-1690, 48-1185).[1]

The structural investigations were carried out using a full-profile structure analysis package (Solovyov, 1998), based on a modified version of the Rietveld (1969) refinement program *DBWS*-9006*PC* (Wiles & Young, 1981). The structure models were determined by Patterson and Fourier synthesis and refined using the Rietveld technique.

Appreciable *hkl*-dependent peak broadening was observed in the powder patterns of all these compounds. In the case of the *cis* isomers the broadening was attributed to the crystallite shape effect. The *hkl* dependence of the FWHM (full-width at half maximum) for the Pearson VII peak function was taken as follows:

$$\mathrm{FWHM}^2 = \mathrm{FWHM}_{\mathrm{iso}}^2 + L_{hkl}^2/\cos(\theta)^2, \quad (1)$$

$$L_{hkl}^2 = (r_1h^2 + r_2k^2 + r_3l^2 + r_4hk + r_5kl + r_6hl)d^2, \quad (2)$$

where $\mathrm{FWHM}_{\mathrm{iso}}$ is a directory-independent value simulated using the Caglioti *et al.* (1958) formula, d is the interplanar spacing of the reflection, and $r_1,...,r_6$ are the adjustable parameters. The reciprocal square root of the quadratic form (2) gives a three-dimensional ellipsoid which represents an average crystallite shape.

The structure investigations of the *trans* and β-*trans* isomers revealed some extra atom positions in the difference Fourier maps. This was interpreted as resulting from the presence of defects in the crystals. Correlations between the occupancies of the extra positions and the indices of the most broadened reflections were found (Kirik *et al.*, 1996). The analysis of these correlations and a pseudosymmetry of the structure macro-elements allowed us to propose a model of the microstructural imperfections for the *trans* and β-*trans* isomers.

[1] Supplementary data for this paper are available from the IUCr electronic archives (Reference: AV0024). Services for accessing these data are described at the back of the journal.

Table 1
Experimental details.

For all compounds, the atomic scattering factors were taken from *DBW*3.2*S*. Computer programs: data collection: *DRON*-4 software; cell refinement and structure refinement: modified Rietveld program *DBWM*; data reduction: *XDIG* (local program); structure solution: local program for Patterson and Fourier synthesis.

	(I)	(II)	(III)	(IV)	(V)
Crystal data					
Chemical formula	*cis*-$[Pd(NH_3)_2Br_2]$	*trans*-$[Pd(NH_3)_2Br_2]$	*β-trans*-$[Pd(NH_3)_2Br_2]$	*cis*-$[Pd(NH_3)_2I_2]$	*β-trans*-$[Pd(NH_3)_2I_2]$
Chemical formula weight	300.29	300.29	300.29	394.29	394.29
Crystal system	Orthorhombic	Triclinic	Orthorhombic	Orthorhombic	Orthorhombic
Space group	*Pbca*	$P\overline{1}$	*Pbca*	*Pbca*	*Pbca*
a (Å)	13.3202 (7)	6.7854 (3)	8.4315 (3)	13.9060 (8)	8.8347 (5)
b (Å)	12.7223 (6)	7.1057 (3)	8.4206 (3)	13.5035 (8)	8.8410 (5)
c (Å)	7.05854 (3)	6.6241 (2)	8.0916 (2)	7.5050 (4)	8.6081 (2)
α (°)	90	103.221 (3)	90	90	90
β (°)	90	102.514 (2)	90	90	90
γ (°)	90	100.386 (3)	90	90	90
V (Å^3)	1196.17 (8)	294.52 (2)	574.49 (4)	1409.29 (9)	672.36 (5)
Z	8	2	4	8	4
Radiation type	Cu $K\alpha$	Cu $K\alpha$	Cu $K\alpha$	Cu $K\alpha$	Cu $K\alpha$
Wavelength (Å)	1.5418	1.5418	1.5418	1.5418	1.5418
Temperature (K)	293	293	293	293	293
Data collection					
Diffractometer	DRON-4 powder	DRON-4 powder	DRON-4 powder	DRON-4 powder	DRON-4 powder
Data collection method	θ–2θ scan	θ–2θ scan	θ–2θ scan	θ–2θ scan	θ–2θ scan
Increment in 2θ (°)	0.02	0.02	0.02	0.02	0.02
2θ range (°)	12–70	12–61	17–75	12–61	17–75
Refinement					
Refinement on	I_{net}	I_{net}	I_{net}	I_{net}	I_{net}
R_p	0.060	0.065	0.069	0.075	0.079
R_{wp}	0.077	0.087	0.091	0.096	0.106
R_{exp}	0.048	0.045	0.048	0.053	0.058
R_B	0.034	0.029	0.037	0.072	0.041
No. of parameters used	43	40	31	38	29
H-atom treatment	H atoms constrained	H atoms constrained	H atoms constrained	H atoms constrained	H atoms constrained
Weighting scheme	Based on measured s.u.'s	Based on measured s.u.'s	Based on measured s.u.'s	Based on measured s.u.'s	Based on measured s.u.'s
Extinction method	None	None	None	None	None

The model includes the presence of stacking faults resulting in multiple twinning of the crystals. The scheme of the twinning is presented in Fig. 1. The twin areas are joined by (001) planes and related to each other by a fourfold axis in *β-trans* (and by a twofold axis in *trans isomers)* perpendicular to the twin plane. The corresponding pseudo-fourfold and pseudo-twofold axes were found to be as the pseudo-symmetry elements in the layers of $[Pd(NH_3)_2X_2]$ complexes parallel to the (001) plane. This pseudo-symmetry makes the stacking faults quite probable allowing two separate layers to join in two different ways, saving the system of intermolecular interactions and, therefore, without substantial change in the crystal energy.

The atomic pseudo-positions derived from the twinning were calculated and found to be in good agreement with the positions of the additional peaks on the Fourier maps. The crystal structure models of the *trans*- and *β-trans* isomers were supplemented by the pseudo-positions and their occupancies were refined simultaneously with the corresponding occupancies of the basic atoms to fix the total content of the unit cell.

The *hkl* dependence of the peak broadening for the *trans*- and *β-trans* compounds was simulated in accordance with the twinning model following the theory described by Solovyov (2000). The Y parameter of the Thompson–Cox–Hastings pseudo-Voigt function (Thompson *et al.*, 1987) used was modified as follows:

$$Y_{hkl} = Y + L_{hkl}2O\left\{1 - \frac{F_oF_1^* + F_1F_o^*}{2[(1-O)|F_o|^2 + O|F_1|^2]}\right\}, \quad (3)$$

where

$$F_o = F_c - O\frac{\partial F_c}{\partial O}, \quad (4)$$

and

$$F_1 = F_c + (1-O)\frac{\partial F_c}{\partial O}, \quad (5)$$

and where F_c is a calculated structure factor of the reflection, O is an overall occupancy of the atomic pseudo-positions and L_{hkl} is the root square of the quadratic form (2). The term L_{hkl} in (3) represents the difference between the length of the twinned areas and the thickness of the crystal in the direction perpendicular to the reflecting plane (Solovyov, 2000).

The application of the anisotropic broadening corrections (1) and (3) permitted a successful structure solution and

Table 2
Fractional atomic coordinates and isotropic displacement parameters (Å^2) for (I).

	Multiplicity	x	y	z	B_{iso}
Pd	8	0.1994 (2)	0.2495 (3)	−0.0433 (3)	1.5 (2)
Br(1)	8	0.0775 (3)	0.3817 (5)	−0.0927 (5)	3.2 (2)
Br(2)	8	0.3306 (3)	0.3771 (4)	0.0101 (5)	2.2 (2)
N(1)	8	0.087 (2)	0.134 (2)	−0.092 (3)	4 (1)
N(2)	8	0.314 (2)	0.153 (2)	−0.002 (2)	1 (1)

refinement with quite satisfactory structural parameters for all the compounds studied. The crystallographic data for $[Pd(NH_3)_2X_2]$, where X = Br or I, are summarized in Tables 1–11. A comparison of experimental and calculated powder patterns is shown in Fig. 2.

3. Results and discussion

The *cis* isomers demonstrate a unique type of structure, while the *trans* and *β-trans* isomers are isostructural to corresponding Cl derivatives (Kirik *et al.*, 1996).

3.1. Crystal structures of *cis*-[Pd(NH$_3$)$_2$(halide)$_2$]

The final Rietveld plot and the crystal structure of *cis*-$[Pd(NH_3)_2Br_2]$ (I) are presented in Figs. 2 and 3, respectively. Virtually planar complexes have the form of a slightly distorted regular trapezoid. The Cl and Br derivatives demonstrate the same type of interatomic distance distortions. Pd—X distances as well as Pd—N ones are not equal. The longest Pd—X distance is opposite the longest Pd—N one. The same situation was observed by Milburn & Truter (1966) for *cis*-$[Pt(NH_3)_2Cl_2]$. The planar complexes are arranged in columns along the *c* axis parallel to one another. In contrast to the Cl compound, where successive molecules in the layer are translationally related by one-side packing, *cis*-$[Pd(NH_3)_2Br_2]$ exhibits double-side molecular packing. The Pd···Pd distances along the column are constant and equal to 3.389 and 3.523 Å. Although these distances are longer than in metal (2.77 Å), it would still be reasonable to consider them as second-order coordination of the Pd atoms. These interactions are probably responsible for the column stability.

Table 3
Selected geometric parameters (Å^2, °) for (I).

Pd—Br(1)	2.363 (6)
Pd—Br(2)	2.414 (5)
Pd—N(1)	2.12 (3)
Pd—N(2)	1.98 (2)
Pd···Pd^{i}	3.529 (3)
Br(1)—Pd—Br(2)	92.4 (3)
N(1)—Pd—N(2)	98 (2)
Br(1)—Pd—N(1)	89 (1)
Br(2)—Pd—N(2)	80.5 (9)

Symmetry codes: (i) $x, \frac{1}{2}-y, z-\frac{1}{2}$.

The comparative column arrangements for Cl and Br compounds are presented in Fig. 4. They follow perfectly the law of compact packing. A more detailed examination of the column net for *cis*-$[Pd(NH_3)_2Br_2]$ reveals a subcell with one eighth of the cell volume and the parameters: a' = 6.502, b' = 6.687, c' = 3.530 Å, α' = 95.3, β' = 90.3, γ' = 102.1°. It almost repeats the unit cell of *cis*-$[Pd(NH_3)_2Cl_2]$. The difference in the molecular packing is probably due to different sterical effects of the Cl and Br atoms.

3.2. Crystal structure of *trans*-[Pd(NH$_3$)$_2$*X*$_2$]

The *trans*-$[Pd(NH_3)_2X_2]$ complexes, where X = Cl or Br, were found to be isostructural. For the iodine derivative, which is unstable and not obtained in a single phase, the formation of the same type of structure was revealed by the X-ray powder diffraction pattern. The molecular structure consists of columns of flat complexes having central symmetry (Kirik *et al.*, 1996). Every second complex in the columns is

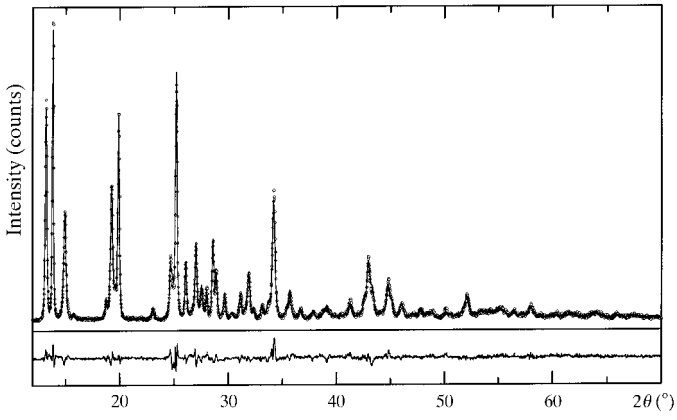

Figure 2
The final Rietveld plot for *cis*-$Pd(NH_3)_2Br_2$.

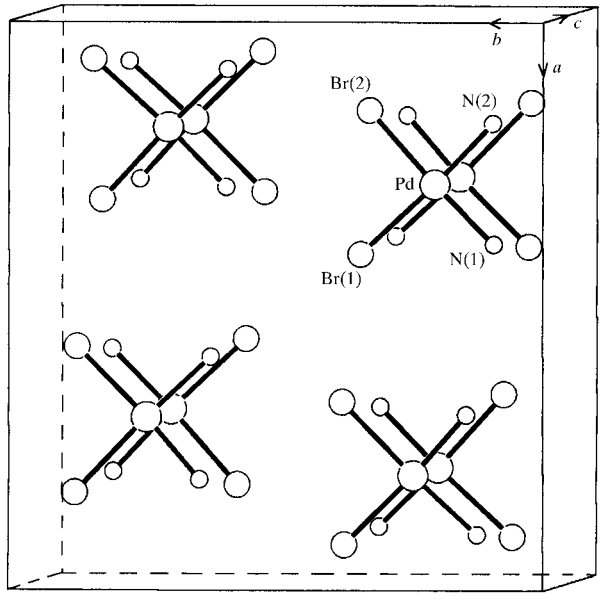

Figure 3
The unit-cell content of *cis*-$Pd(NH_3)_2Br_2$

Table 4
Fractional atomic coordinates and isotropic displacement parameters (Å^2) for (II).

	Multiplicity	Occupancy	x	y	z	B_{iso}
Pd(1)	1	0.896 (3)	0	0	0	0.9 (1)
Pd(2)	1	0.896 (3)	0	1/2	0	0.9 (1)
Pd(3)	2	0.026 (3)	0.08	0.08	0	0.9 (1)
Pd(4)	2	0.026 (3)	0.08	0.58	0	0.9 (1)
Pd(5)	2	0.026 (3)	0.54	0.04	0	0.9 (1)
Pd(6)	2	0.026 (3)	0.54	0.54	0	0.9 (1)
Br(1)	2	0.896 (3)	−0.2009 (8)	0.0691 (1)	0.2608 (8)	1.8 (1)
Br(2)	2	0.896 (3)	0.3284 (8)	0.571 (1)	0.2721 (6)	1.8 (1)
Br(3)	2	0.052 (3)	−0.1409 (8)	0.129 (1)	0.2608 (8)	1.8 (1)
Br(4)	2	0.052 (3)	0.3884 (8)	0.631 (1)	0.2721 (6)	1.8 (1)
Br(5)	2	0.052 (3)	−0.2609 (8)	0.009 (1)	0.2608 (8)	1.8 (1)
Br(6)	2	0.052 (3)	0.2684 (8)	0.511 (1)	0.2721 (6)	1.8 (1)
N(1)	2	1	0.278 (4)	0.072 (5)	0.227 (3)	4.3 (5)
N(2)	2	1	−0.156 (4)	0.550 (4)	0.241 (4)	4.3 (5)

Table 5
Selected geometric parameters (Å^2, °) for (II).

Pd(1)—Br(1)	2.441 (5)
Pd(2)—Br(2)	2.430 (5)
Pd(1)—N(1)	2.04 (2)
Pd(2)—N(2)	2.10 (5)
Pd(1)—Pd(2)	3.5529 (2)
Br(1)—Pd(1)—N(1)	94 (1)
Br(2)—Pd(2)—N(2)	90 (1)

rotated at nearly 90° with respect to the first. Although the complexes are symmetrically independent, their geometry is very similar. The Pd···Pd distances (3.4285 Å for Cl complex and 3.553 Å for Br complex) are greater than for the corresponding *cis* isomers. This is probably due to the stronger long distance affinity for the *cis* isomer rather than for the *trans* isomer. Crystal defects of the stacking fault type are inherent in both Cl and Br *trans* isomers.

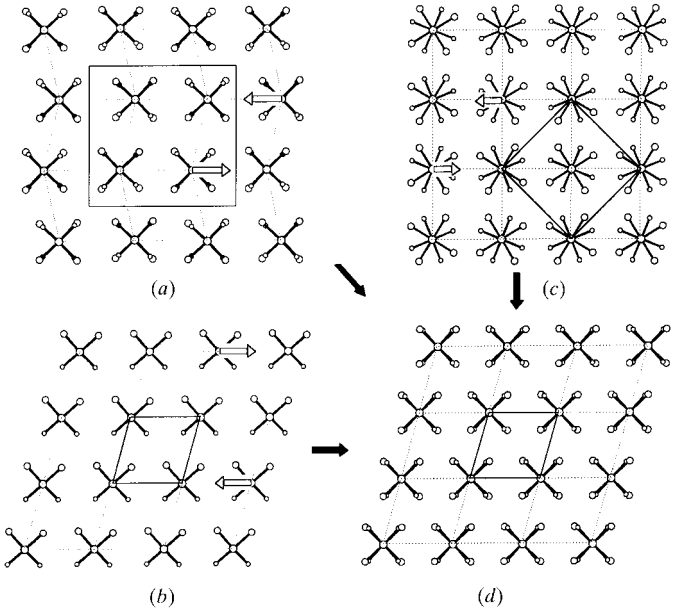

Figure 4
Column arrangement in (*a*) *cis*-$[Pd(NH_3)_2X_2]$, (X = Br, I), (*b*) *cis*-$[Pd(NH_3)_2Cl_2]$, (*c*) $[Pd(NH_3)_4][PdX_4]$ and (*d*) *trans*-$[Pd(NH_3)_2X_2]$. The unit cells are indicated by solid lines. The translations for the columns of layers, providing transformations into *trans*-$[Pd(NH_3)_2X_2]$, are pointed out by empty arrows.

3.3. Crystal structure of *β-trans*-$[Pd(NH_3)_2X_2]$

A complete analogy in the crystal structures of Cl, Br and I derivatives for the *β-trans* form was found. The pseudo-tetragonal cell characterizes all of the compounds studied. The geometry of the molecules in *trans* and *β-trans* isomers is quite similar, but the molecular arrangements are different. The Pd atoms in the *β-trans* isomer principally change their long distance coordination. Instead of Pd atoms of neighbouring complexes, halide atoms play the roles of additional tops to form an octahedron surrounding. This circumstance strongly influences the type of molecular packing. Here $[Pd(NH_3)_2X_2]$ complexes are joined through the Pd···halide contacts in the layers with a parquet-like packing. The layers are linked by a system of hydrogen bonds. The most probable hydrogen bonds were found by analysis of the geometry. The structure is considered to be a layered type influenced by an order–disorder phenomenon. This is a common feature for all *trans*-$[Pd(NH_3)_2X_2]$. The layer orientation appears to be quite easily changed by an angle of $\pi/2$ (Kirik *et al.*, 1996). It has been mentioned already that the one-dimensional disordering along the *c* axis reveals itself in anisotropic peak broadening and also in the appearance of pseudo-atomic positions.

The negative value of B_{iso} for N atoms in *β-trans*-$[Pd(NH_3)_2I_2]$, (Table 10) can be commented as a calculating effect due to the application of an isotropic thermal factor in the description of the heavy atoms.

3.4. Phase transitions in $[Pd(NH_3)_2X_2]$

Structural investigations of a series of compounds with similar formulae can provide a new background for more substantial considerations of the thermal stability and transformation of palladium aminohalogens. Previous data on the subject were obtained by thermal analysis (Kukushkin *et al.*, 1981). Some considerations concerning transformations in $[Pd(NH_3)_2Cl_2]$, based on structural data, were presented in a previous paper by the authors (Kirik *et al.*, 1996).

The *cis–trans* transformation is a special type of chemical reaction with an extremely limited degree of chemical transport through the substance. It is of special interest because of the opportunity to observe a chemical reaction in the solid state. The process can be considered as a chemical reaction because of the substantial changes in chemical bonding, which is responsible for the transformation. It was already noted that thermal transformation in $[Pd(NH_3)_2Cl_2]$ in a bulk sample

Table 6
Fractional atomic coordinates and isotropic displacement parameters (Å^2) for (III).

	Multiplicity	Occupancy	x	y	z	B_{iso}
Pd	4	1	0	0	0	0.80 (8)
Br(1)	8	0.946 (3)	0.2065 (2)	0.2031 (2)	0.0060 (7)	1.63 (9)
Br(2)	8	0.054 (3)	−0.2031 (2)	0.2065 (2)	−0.0060 (7)	1.63 (9)
N	8	1	0.014 (4)	0.030 (2)	0.2515 (8)	0.5 (3)

Table 7
Selected geometric parameters (Å^2, °) for (III).

Pd—Br(1)	2.440 (2)
Pd—N	2.053 (7)
Pd^{i}—Br(1)	3.519 (2)
Br(1)—Pd—N	82 (1)

Symmetry codes: (i) $\frac{1}{2}-x, \frac{1}{2}+y, z$.

Table 8
Fractional atomic coordinates and isotropic displacement parameters (Å^2) for (IV).

	Multiplicity	x	y	z	B_{iso}
Pd	8	0.2048 (3)	0.2463 (4)	−0.0353 (8)	1.5
I(1)	8	0.0771 (3)	0.3795 (5)	−0.0995 (6)	1.5
I(2)	8	0.3311 (2)	0.3789 (4)	0.0450 (7)	1.5
N(1)	8	0.118 (2)	0.124 (4)	−0.121 (5)	1.5
N(2)	8	0.310 (2)	0.134 (3)	0.028 (5)	1.5

Table 9
Selected geometric parameters (Å^2, °) for (IV).

Pd—I(1)	2.573 (7)
Pd—I(2)	2.580 (7)
Pd—N(1)	2.14 (5)
Pd—N(2)	2.16 (4)
Pd—Pd^{i}	3.754 (9)
I(1)—Pd—I(2)	91.6 (3)
N(1)—Pd—N(2)	85 (2)
I(1)—Pd—N(1)	95 (2)
I(2)—Pd—N(2)	89 (2)

Symmetry codes: (i) $x, \frac{1}{2}-y, z-\frac{1}{2}$.

occurs at increasing temperatures through *cis*→*trans*→*β-trans* structures with decreasing specific volume. This rather unusual behaviour was also found for $[Pd(NH_3)_2Br_2]$, and it differentiates such a process from an ordinary phase transition. The *trans*→*β-trans* transformation deserves a special comment. The geometry of molecular complexes remains practically the same. The decrease in specific volume in this case can be related to the formation of new long-length-scale chemical interactions of Pd atoms perpendicular to the complex planes.

To understand the kinetic and thermodynamic relations between isomers, the results of some additional experiments should be discussed. The transformation of *cis*-$[Pd(NH_3)_2Br_2]$ was studied by high temperature X-ray diffraction using a thin layer of sample in air. The rate at which the *cis* isomer transformed into the *trans* one was noticeable at 400 K. Due to the differences in powder patterns of the isomers it was easy to observe a gradual change of one phase into the other. Traces of the *β-trans* isomer were detected as a side product of the transformation. Then the decomposition of *trans*-$[Pd(NH_3)_2Br_2]$ occurs at 440 K in two parallel processes yielding $PdBr_2$ and Pd metal. It should be mentioned that the *β-trans* isomer can be obtained from the *trans* one by the thermal treatment of a bulk sample at 460 K (Smirnov *et al.*, 1981). Thus, there was an obvious difference between the transformation of a thin layer and bulk sample. The transformation schemes of Br and Cl derivatives are quite similar and differ only at the final stages.

The thermodynamic relation for *trans* and *β-trans* isomers was investigated for the Cl derivative. It was found that the equilibrium between *trans* and *β-trans* phases could be achieved approximately at 290 K when the substance was placed in water for a few days. At temperatures lower than 290 K, the substance should be in the form of the *trans* isomer and above this temperature it could convert to the *β-trans* form. Thus, the thermodynamically expected phase at 400 K is the *β-trans* isomer. This means that the transformation of *cis* into *trans* at 400 K in the thin layer sample follows more the kinetics rather than the thermodynamic regularities. Further transformation into the *β-trans* phase was not observed. Recrystallization into the *β-trans* phase probably requires that some partial pressure of the sublimed product vapours be maintained above the sample surface. Formation of the *β-trans* isomer in a bulk sample occurs since such favourable conditions are likely to be realised in a large volume of the substance.

The process is close to the thermal transformation of Vokelen's salts $[Pd(NH_3)_4][PdX_4]$. According to Kukushkin *et al.* (1974), Vokelen's salts transformed into *trans*-$[Pd(NH_3)_2X_2]$ approximately at the same temperature as further decomposition. This was confirmed by their experiments on the basis of differential thermal and gravimetric analysis. The molecular mechanism of this solid-state reaction was presented as a synchronized shift of the ligands along the metal columns.

Thus, three geometrically different structures, namely *cis*-$[Pd(NH_3)_2Cl_2]$, *cis*-$[Pd(NH_3)_2Br_2]$ and $[Pd(NH_3)_4][PdX_4]$ convert into the structure of *trans*-$[Pd(NH_3)_2X_2]$. The transformation occurs at 400 K, as controlled by kinetics. Taking all this together, we proposed that the process can proceed in the solid without crystals being destroyed. This hypothesis makes rational the formation of the thermodynamically unstable *trans* isomer.

It follows that an important feature of the transformation should be that it goes *via* the breaking of some interatomic bonds (Pd—N or Pd—*X*). The breaking of bonds is necessary for the transformation of $[Pd(NH_3)_4][PdX_4]$ into *trans*-$[Pd(NH_3)_2X_2]$. As for *cis* compounds, this argument is not so clear. However, the same temperature and pressure conditions

Table 10
Fractional atomic coordinates and isotropic displacement parameters (Å^2) for (V).

	Multiplicity	Occupancy	x	y	z	B_{iso}
Pd	4	1	0	0	0	1.28 (8)
I(1)	8	0.963 (3)	0.2121 (2)	0.2076 (2)	−0.0095 (4)	1.71 (8)
I(2)	8	0.037(3)	−0.2076 (2)	0.2121 (2)	0.0095 (4)	1.71 (8)
N	8	1	0.052 (3)	0.017 (5)	0.234 (1)	−3.4 (6)

Table 11
Selected geometric parameters (Å^2, °) for (V).

Pd—I(1)	2.624 (2)
Pd—N	2.07 (1)
Pd^{i}—I(1)	3.628 (2)
I(1)—Pd—N	80 (1)

Symmetry codes: (i) $\frac{1}{2}-x, \frac{1}{2}+y, z$.

and the sterical difficulty for molecular flopping in the vicinity of crystals are strong arguments for bond breaking. The metal columns ($M\cdots M$ contacts) remain intact in the process of transformation. To transform every starting structure into *trans*-$[Pd(NH_3)_2X_2]$ in the solid, whole layers of columns have to shift relative to one another. Possible column shifts are shown in Fig. 4 by arrows. All shifts are similar, but apply to different layers. Combinations of two or three layers are involved in the transformation. For $[Pd(NH_3)_2Cl_2]$, there are two options for the lattice to become geometrically close to the *trans* isomer: to shift every second layer along **a** by half of a translation or without any shift. For *cis*-$[Pd(NH_3)_2Br_2]$, two column layers are subjected to the shift by half a translation. In the case of $[Pd(NH_3)_4][Pd(halide)_4]$, the required column displacement may be achieved by shifting two layers by 1/3**a**. The chemical process of transformation spreads through the crystal by a front, which is parallel to the metal columns. The specific microstructural imperfection detected in *trans*–$[Pd(NH_3)_2(halide)_2]$ is in the agreement with these possible processes taking place in the crystals.

The driving force of this transformation is an alteration of palladium electronic structure. This transformation is irreversible at 400 K and goes through an intermediate stage. After *cis*→*trans* isomerization, the co-axial $M\cdots M$ contacts are not so energetically favourable as $Pd\cdots X$. To establish new contacts, the crystal structure has to be destroyed. This requires overcoming a high energy activation barrier. This is the reason why the *cis* isomer converts into the thermodynamically unfavourable *trans* one.

Thus, if this mechanism of transformation is correct, the following conclusions can be made. The transformation observed shows the importance of long-range co-axial Pd···Pd contacts. The *cis* configuration prefers electron deficient neighbours, while the *trans* isomer prefers neighbours having excess electron density. The *cis* compounds demonstrate kinetic stability in the solid state. The *cis–trans* transformation occurs through the breaking of Pd—N or Pd—X bonds. Therefore, it may be classified as an S_N1-like mechanism.

The authors would like to thank ICDD (grant N93-10) and Krasnoyarsk Regional Science Foundation (grant 6 F0178) for their financial support.

References

Caglioti, G., Paoletti, A. & Ricci, F. P. (1958). *Nucl. Instrum.* **3**, 223–228.
Kirik, S. D., Borisov, S. V. & Fedorov, V. E. (1979). *Zh. Strukt. Khimii*, **20**, 359. (In Russian.)
Kirik, S. D., Solovyov, L. A., Blokhin, A. I., Yakimov, I. S. & Blokhina, M. L. (1996). *Acta Cryst.* B**52**, 909–916.
Kukushkin, Yu. N., Budanova, B. F. & Sedova, G. N. (1981). *Termocheskoe prevraschenie koordinatsionnych soedinenii v tverdom tele*. Leningrad: LGU.
Kukushkin, Yu. N., Krylova, T. C. & Bakhireva, S. I. (1974). *Zh. Neorg. Khimii*, **19**, 1694–1696.
Milburn, G. H. & Truter, M. R. (1966). *J. Chem. Soc. A*, **11**, 1609–1616.
Porai-Koshits, M. A. (1954). *Tr. Inst. Kristallogr. Akad. Nauk SSSR*, **9**, 229–238.
Rietveld, H. M. (1969). *J. Appl. Cryst.* **2**, 65–71.
Smirnov, I. I., Volkova, G. V., Chumakov, V. G. & Volkov, V. E. (1981). *Zh. Neorg. Khimii*, **26**, 2859–2861.
Solovyov, L. A. (1998). Personal communication.
Solovyov, L. A. (2000). *J. Appl. Cryst.* **33**, 338–343.
Thompson, P., Cox, D. E. & Hastings, J. B. (1987). *J. Appl. Cryst.* **20**, 79–83.
Visser, J. W. (1969). *J. Appl. Cryst.* **2**, 89–95.
Wiles, D. B. & Young, R. A. (1981). *J. Appl. Cryst.* **14**, 149–151.